Spring 5-29-2024

IMMUNE RESPONSES OF NEONATAL (14-DAY OLD) AND ADULT (6 WEEKS OLD) MICE LUNG AND SPLEEN CELLS TO GAMMA-IRRADIATED MYCOBACTERIUM TUBERCULOSIS STIMULATION

Oyinkansola F. Adeyemi
University of Texas Health Center at Tyler, oadeyemi@patriots.uttyler.edu

IMMUNE RESPONSES OF NEONATAL (14-DAY OLD) AND ADULT (6 WEEKS OLD) MICE LUNG AND SPLEEN CELLS TO GAMMA-IRRADIATED MYCOBACTERIUM TUBERCULOSIS STIMULATION

By

OYINKANSOLA FAITH ADEYEMI

A thesis submitted in partial fulfillment of
the requirements for the degree of
Master of Science in Biotechnology
Department of Cellular and Molecular Biology
Ramakrishna Vankayalapati, Ph.D. Thesis Director
School of Medicine

The University of Texas at Tyler

MAY 2024

The University of Texas at Tyler
Tyler, Texas

This is to certify that the Master's Thesis of

OYINKANSOLA FAITH ADEYEMI

has been approved for the thesis requirement on
April 26, 2024 for
the Master of Science in Biotechnology degree

Approvals:

V. Ramakrishna

Rama krishna Vankayalapati,Ph.D, Thesis Director

Vijay Boggaram

Vijay Boggaram, Ph.D, Committee Chair

Pierre Neuenschwander, Ph.d, Committee Member

Buka Samten

Buka Samten, MD , Committee Member

Mitsuo Ikebe, PhD, Chair,
Cellular and Molecular Biology

Brigham Willis, M.D., Dean,
School of Medicine

ABSTRACT

Tuberculosis (TB) caused by *Mycobacterium tuberculosis* (Mtb) is a global health challenge, especially in vulnerable populations like neonates, whose immune systems are still developing. Understanding the immune responses to *Mtb* in neonates is critical for the development of better vaccine and treatment strategies. Building upon previous research from our laboratory, which demonstrated that *γMtb* stimulated neonatal mice (0, 3, and 7 days old) lung cells displayed distinct cytokine profiles and increased expansion of myeloid-derived suppressor cell subpopulations than adult mice lung cells. In the current study, we investigated age-dependent immune responses in 14-day-old (neonates) and 6-week-old (adults) mice. We found that IL-6, TNF-α, and IL-10 cytokine levels were significantly higher in *γMtb* stimulated neonatal lung cell culture supernatants than in unstimulated controls and adult mice lung cells stimulated with *γMtb.* CD45+CD4+CD8+ cell population was significantly higher and CD11c+MHCII+ and NK1.1+ cell populations were lower in freshly isolated lung cells of neonatal mice than in adult mice lung cells. *γMtb* stimulated neonatal lung cells had a higher percentage of CD11b+Ly6G+, CD4+, and CD4+CD69+ cell population and lower levels of NK1.1+ and B cell populations than in *γMtb* stimulated adult lung cells. Overall, our study demonstrated that neonatal and adult mice immune cells respond differently to *γMtb* stimulation. These findings enhance our understanding

of age-related variations in host immune responses and may help guide the development of targeted interventions to combat TB, particularly in newborns.

ACKNOWLEDGMENTS

I am deeply grateful to Professor Ramakrishna Vankayalapati, my thesis advisor, for his unwavering patience and guidance throughout this journey. Professor Vijay Boggaram, my thesis committee chairman, Professor Buka Samten, as a committee member, and Professor Pierre Neuenschwander as a committee member, provided invaluable feedback that shaped this endeavor. I owe a debt of gratitude to Research Assistant Professor Rajesh Kumar Radhakrishnan for his generous sharing of knowledge and expertise.

My research was enriched by the collaboration of remarkable individuals. I extend my heartfelt thanks to my laboratory colleagues, particularly Olamipejo Durojaye, Tanmoy Mukherjee, and Bismark Owusu-Afriyie, for their steadfast support. I am also indebted to the wise advice of Professor Torry Tucker, Professor Amy Tvinnereim, and Professor Mitsuo Ikebe.

None of this would have been possible without the generous funding from the Biotechnology Program and the unwavering support of program coordinators and administrative staff. I am grateful for the friendship and inspiration provided by my classmates and fellow MS Biotechnology students at UT Tyler Health Science Center from 2022 to 2024.

Lastly, I extend special thanks and recognition to my family, particularly my sister, Ms Aderinsola Adeyemi, and my parents, Engr. Ademola Adeyemi and Mrs Olufunmilayo Adeyemi. Their unwavering belief in me and their enduring emotional support were my pillars throughout my studies.

TABLE OF CONTENTS

LIST OF FIGURES

LIST OF TABLES

LIST OF ABBREVIATIONS

TNF-α: Tumor Necrosis Factor Alpha

PBS: Phosphate-buffered saline

PBST: Phosphate-Buffered Saline Tween-20

HBSS: Hank's Balanced Salt Solution

RPMI: Roswell Park Memorial Institute 1640

***Mtb*:** *Mycobacterium tuberculosis*

TB: Tuberculosis

qRT-PCR: Quantitative Real-time Polymerase Chain Reaction

RNA: Ribonucleic Acid

***γMtb*:** Gamma-Irradiated *Mtb*

LDH: Lactate dehydrogenase

ELISA: Enzyme-linked immunosorbent assay

INTRODUCTION

Tuberculosis (TB) caused by *Mycobacterium tuberculosis* (Mtb), remains a significant global health concern, particularly in developing regions [1]. The immune system plays a vital role in the control of *Mtb* infection [2]. Age-related variations in immune function can significantly impact susceptibility to infectious diseases, including TB [3]. Children, especially those younger than five years, are more susceptible to tuberculosis (TB) infection due to an immature immune system [4]. It is difficult to diagnose TB in children especially children younger than 5 years [4]. Early diagnosis of TB infection in children who are at increased risk for its development would allow treatment of high-risk children [5]. To develop diagnostic markers for early TB diagnosis, a detailed understanding of the immune responses in children infected with *Mtb* is essential [6] [7]. Animal models, especially the neonatal mouse model of *Mtb* infection, help understand immune responses. Adult mice have been extensively studied in the TB research [8]. However, limited information is available about the immune responses of neonatal mice infected with *Mtb* [9].

Neonates have an immune system that is developing which increases their vulnerability to infections [10]. Exploring the distinct immune responses between these two age groups will contribute to a more comprehensive understanding of the TB pathogenesis [11] and the immune mechanisms underlying disease progression in children. Moreover, deciphering the natural immunity conferred by adult and neonatal mice can provide valuable insights into the development of potential preventive strategies and therapeutic interventions [10]. By elucidating the

mechanisms that contribute to enhanced or compromised immune responses, we can identify novel targets for intervention and formulate age-specific approaches to combat TB effectively.

Cytokines play a crucial role in orchestrating immune responses against mycobacterial pathogens [12]. They regulate the activation of immune cells [13], influencing the balance between protective immunity and pathological damage. Understanding the specific cytokine profiles associated with different age groups during TB infection is essential for unraveling the intricate dynamics of host-pathogen interactions. Previous studies have shown that adult mice possess more robust host-beneficial immune responses. These are characterized by increased production of pro-inflammatory cytokines, such as tumor necrosis factor-alpha (TNF-α) and interferon-gamma (IFN-γ), as well as efficient activation of macrophages and T lymphocytes [14], [15]. Recent studies demonstrated that infant and adult alveolar macrophages infected with *Mtb* H37Rv have similar phagocytic capacity, but infant alveolar macrophages were unable to control bacterial replication [16]. Likewise, both infant and adult macrophages infected with *Mtb* produce similar levels of pro- and anti-inflammatory cytokines production, however, infants' alveolar macrophages infected with *Mtb* are defective in antimycobacterial activity and IFN-γ induction signaling pathways [16]. However, the immune responses of neonatal mice, which are still in the initial stages of immune system development, remain poorly understood.

Our laboratory recently developed a neonatal mouse model of *Mtb* infection. Our unpublished studies demonstrate that neonatal mice are more susceptible to

Mtb infection than adult mice. In the current study, we compared the immune response of neonatal mice (14-day-old) with adult mice (6 weeks old) lung and spleen cells stimulated with *γMtb*. The findings of this study will not only add to the existing body of knowledge on TB immunology but also serve as a foundation for future studies aimed at developing age-targeted interventions to combat this formidable disease.

RESEARCH HYPOTHESIS

We tested the hypothesis that neonatal mice (14-day old) immune cells produce higher levels of inflammatory cytokines than adult (6-weeks old) mice immune cells in response to *γMtb* stimulation due to an immature immune system and hyperactivation of immune cells. We also hypothesized that *γMtb* stimulated neonatal and adult mice immune cells would have different immunophenotypes.

Experimental Objectives

1. To compare immunophenotypes between unstimulated controls and *γMtb* stimulated neonatal and adult mice lung and spleen cells in vitro.
2. To compare cytokine profiles between unstimulated controls and *γMtb* stimulated neonatal and adult mice lung and spleen cells in vitro.

MATERIALS AND METHODS

Materials

Deionized water, 1X Phosphate-buffered saline (PBS; SIGMA®), gamma irradiated-*Mtb (γMtb)* (BEI resources), collagenase A (Roche), dispase (FisherScientific), DNASE 1 (Fisher Scientific), 40 µm nylon mesh (Fisherbrand), petri dishes (Fisherbrand), 0.4% Trypan blue solution (Amresco), 1X Complete Roswell Park Memorial Institute media (1% Penicillin/Streptomycin + 1% Sodium pyruvate + 10% Fetal Bovine Serum), bovine serum albumin (Fisher bioreagents), NalgenTM rapid flow filter unit (Thermo Scientific), Phosphate-buffered saline tween-20 (PBST) buffer powder (QuickSILVER); 70% EtOH, conical tubes, 1x red blood cells lysis buffer (Sigma Aldrich), mouse IL-6, IL-10, IL-17A, TNF-α and IFN-γ ELISA kits (BioLegend®), 1x versene, LIVE/DEAD fixable aqua dead cell stain kit (Invitrogen), cell surface flow cytometry antibody markers (CD45, CD4, CD8, CD25, CD69, MHCII, CD11b, CD11c, Ly6G, Ly6C, F4/80, NK1.1, CD3, LY49A, B220) CyQUANT^{TM} LDH Cytotoxicity Assay kit (Thermo Fisher) and 1% paraformaldehyde.

Reagent Preparation

a) 1X PBST was prepared by adding 1L deionized water to one packet of PBST buffer powder. The mixture was stirred until the powder dissolved completely.
b) 1x Cell staining buffer was prepared using 1x PBS containing 2% heat-inactivated FBS.

c) Complete culture medium was prepared by adding 2.5 ml 100x Penicillin/Streptomycin (antibiotic; final concentration of 1x), 2.5 ml of sodium pyruvate, and 25 ml Fetal Bovine Serum to 220 ml of Roswell Park Memorial Institute media 1640.

Animals

Specific pathogen-free 14-day-old and 6-week-old C57BL/6 male and female mice were used for the study. All experiments were performed with approval from the Institutional Animal Care and Use Committee (IACUC) of the University of Texas at Tyler Health Science Center. The mice were housed under a 12h light/12h dark cycle and fed standard mouse chow and provided water.

Isolation and culture of mouse spleen and lung cells

Murine spleen and lung cells were isolated from 14-day-old and 6-week-old mice. Briefly, mice were euthanized by CO_2 asphyxiation followed by cervical dislocation, then placed in a supine position on a clean dissection surface. The fur was moistened with 70% ethanol to maintain sterility and a midline incision was made in the abdomen using scissors to expose the peritoneal cavity. The spleen, which is a dark-red organ on the left side of the abdomen was then located and gently lifted using forceps and carefully separated from surrounding tissues. Any connective tissues or fat attached to the spleen were trimmed and the isolated spleen was placed in a collection tube on ice.

The harvested spleens were homogenized and filtered through a 40µm nylon cell strainer and 1x HBSS was added to a final volume of 10 ml. Cells were pelleted by centrifugation at 350 x g for 10 minutes at room temperature. The supernatant was discarded, and the pellets were resuspended in 1 ml of Red Blood Cell lysis buffer for 1 minute, after which HBSS was added to a volume of 10 ml. Cells were pelleted by centrifugation at 350 x g for 10 minutes. The supernatant was then discarded, and the pellets were resuspended in a complete RPMI 1640 medium for cell counting and culture.

For in vitro antigen stimulation experiments, 1×10^6 cells/well in 24 well plates were cultured with or without 10 µg/mL of *γMtb* at 37°C in a humidified atmosphere of 95% room air and 5% CO_2 for 72 hours.

For Isolation of the lungs, after exposing the peritoneal cavity, the diaphragm, which separates the abdominal and thoracic cavities was located and an incision was made in the diaphragm to access the thoracic cavity. The lungs were identified, and each lung lobe was gently lifted using forceps and carefully separated from the surrounding tissues. Any connective tissues or fat attached to the lung lobe was trimmed. The isolated lung lobes were then placed in a collection tube on ice.

Harvested lungs were cut into pieces and incubated in 500 µl enzyme-tissue digestion buffer (Enzyme-tissue digestion buffer: 0.25% collagenase A, 20% dispase, 1.25% DNASE 1 in 1X RPMI 1640 medium in cell culture incubator) for 30 minutes. It was then homogenized and filtered through a 40µm nylon cell strainer and HBSS was added to a final volume of 10 ml. Cells were pelleted by centrifugation at 350 x g for 10 minutes at room temperature. The supernatants were

discarded, and the pellets were resuspended in 1 ml of Red Blood Cell lysis buffer for 1 minute, after which HBSS was added to a volume of 10 ml. Cells were pelleted by centrifugation at 350 x g for 10 minutes. The supernatant was then discarded, and the pellets were resuspended in a complete RPMI 1640 medium for cell counting and culture.

For in vitro antigen stimulation experiments, 1 $\times 10^6$ cells/well in 24 well plates were cultured with or without 10 µg/mL of *γMtb* for 72 hours.

Cells were collected for flow cytometry staining using 1x versene. The culture supernatants were collected and stored at -80°C for cytokine analysis and LDH assay.

Gamma-irradiated *Mtb* (*γMtb*) was used throughout this study to stimulate spleen and lung cells. Gamma-irradiation of *Mtb* effectively inactivates its replicative capacity while preserving its antigenic properties, making it suitable for studying host immune responses without the risk of causing active infection. Gamma-irradiation of *Mtb* was obtained from BEI Resources NR-49098.

ELISA and LDH assay

Cell culture supernatants from the above-mentioned experiments were collected after 72 h and stored at −80 °C. The concentrations of TNF-*α*, IL-6, IL-10, IL-17A, and INF-*γ* were measured by enzyme-linked immunosorbent assay (ELISA) and effects on cell toxicity were measured by LDH assay according to the manufacturer's protocols.

Flow cytometry

Cultured cells were lifted using 1x versene and washed with 1x HBSS. Cells were stained with Live/Dead Aqua staining for 30 mins at 4°c and washed with 1x HBSS. For surface staining, live/dead stained cells were resuspended in 200 µL staining buffer (PBS containing 2% heat-inactivated FBS) and incubated at 4°C for 30 minutes with appropriate cell surface staining antibodies (**Tables 1, 2, 3**), washed twice, and fixed in 1% paraformaldehyde (Millipore Sigma) before flow cytometry analysis using Attune NxT acoustic flow cytometer (Invitrogen). Flow cytometry data was analyzed using FlowJo version 10.8.1 software.

Table 1: T Cell Panel.
Cell surface markers, fluorophores, and channels for checking the cell populations of isolated T cells.

CATALOG #	ANTIBODY WITH FLUOROPHORE	ATTUNE LASER
BioLegend 103140	BV 605 anti-mouse CD45 Antibody	VL3
BioLegend100408	PE anti-mouse CD4 Antibody	YL1
BioLegend 100748	APC anti-mouse CD8 Anti-body	RL1
BioLegend 101912	PerCP/Cyanine5.5 anti-mouse CD25 Antibody	BL3
BioLegend 104526	APC/Cyanine7 anti-mouse CD69 Antibody	RL3
INVITROGEN	LIVE/DEAD - Aqua	VL2

Table 2: NK Cell Panel.
Cell surface markers, fluorophores, and channels for checking the cell populations of isolated NK cells.

CATALOG #	ANTIBODY WITH FLUOROPHORE	ATTUNE LASER
BioLegend 103140	BV 605 anti-mouse CD45 Antibody	VL3
BioLegend 100220	PE/Cyanine7 anti-mouse CD3 Antibody	YL4
BioLegend 108748	PE/Dazzle anti-mouse NK1.1 Antibody	YL2
BioLegend 104508	PE anti-mouse CD69 Antibody	YL1
BioLegend 116810	Pacific Blue anti-mouse Ly49A Antibody	VL1
BioLegend 103212	APC anti-mouse/human CD45R/B220 Antibody	RL1
INVITROGEN	LIVE/DEAD - Aqua	VL2

Table 3: Myeloid Cell Panel.
Cell surface markers, fluorophores, and channels for checking the cell populations of isolated Myeloid cells.

CATALOG #	ANTIBODY WITH FLUOROPHORE	ATTUNE LASER
BioLegend 103140	BV 605 Anti-Mouse CD45 Antibody	VL3
BioLegend 107606	FITC Anti-Mouse MHCII (I-A/I-E) Antibody	BL1
BioLegend 126622	PE/Dazzle Anti-Mouse CD11b Antibody	YL2
BioLegend 117324	APC/Cyanine7 Anti-Mouse CD11c Antibody	RL3
BioLegend 127614	APC Anti-Mouse LY-6G Antibody	RL1
BioLegend 128008	PE Anti-Mouse LY-6C Antibody	YL1
BioLegend 123114	PE/Cyanine7 Anti-Mouse F4/80 Antibody	YL4
BioLegend 108732	BV421 Anti-Mouse NK1.1	VL1
INVITROGEN	Live/Dead - Aqua	VL2

Statistical Analysis

All data analysis was conducted using GraphPad Prism 9.0 (GraphPad Software Inc.) and all results were expressed as the mean ± standard deviation (SD).

For normally distributed data, an unpaired t-test was performed to compare between groups. One-way ANOVA followed by Tukey's test for multiple comparisons was performed. $p < 0.05$ was considered significant.

Power analysis

The minimum number of mice required for experiments was determined by statistical power analysis. For power calculations (http://www.rad.jhmi.edu/jeng/javarad/samplesize/), we assumed that data would be normally distributed among unstimulated control and *γMtb* stimulated mice lung and spleen cells (in vitro). Power analysis was performed using the following parameters, the difference between control and *γMtb* stimulated mice lung and spleen cells is 60%, the estimated standard deviation is 20%, the desired power is 90% and the significance criterion is 0.05. From this power analysis, we required 4.7 mice (~5 mice) for each group.

RESULTS

Comparison of body, lung, and spleen weights of adult (6 weeks old) and neonatal mice (14-day old)

The body weight and wet weight of the lungs and spleens of twelve mice (three 14-day-old male and three 14-day-old female mice and three 6-weeks old male and three 6-weeks old female mice) were compared (**Table 4 and Fig. 1**). The analysis of body weight, lung weight, and spleen weight showed that adult mice exhibited statistically significantly higher weights than neonates across all measured parameters.

Table 4: Body and organ weights of neonatal and adult mice.

MICE IDENTIFICATION	LUNG (mg)	SPLEEN (mg)	BODY WEIGHT (g)
ADULT MALE 1	209.7	80.5	23.8
ADULT MALE 2	354.0	67.9	20.46
ADULT MALE 3	338.3	80.4	24.09
ADULT FEMALE 1	200	98	17.4
ADULT FEMALE 2	182.8	65.1	17.73
ADULT FEMALE 3	322.1	50	16.01
NEONATAL MALE 1	177.7	38.2	7.97
NEONATAL MALE 2	161.7	47.3	6.51
NEONATAL MALE 3	180.6	52.8	7.42
NEONATAL FEMALE 1	172.4	42.1	7.88
NEONATAL FEMALE 2	156.1	34.4	7.50
NEONATAL FEMALE 3	163.8	43.7	6.8

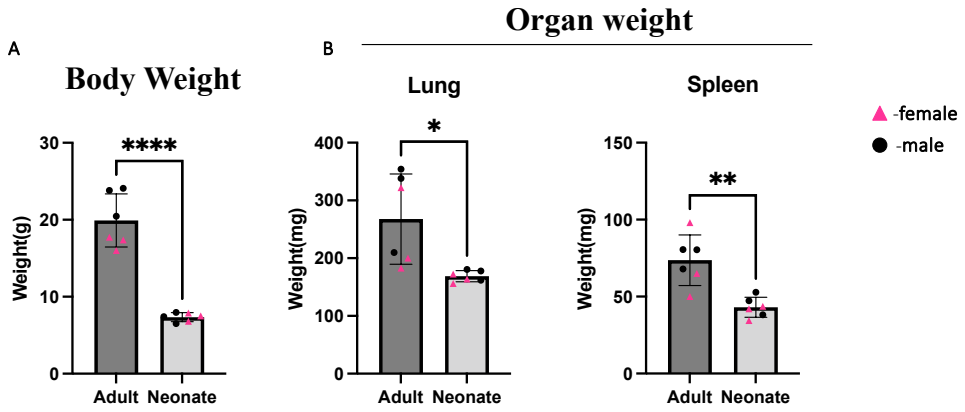

Figure 1: Comparison of body and organ weights of adult and neonatal mice.
Twelve pathogen free C57BL/6 mice (three 14-day old male and three 14-day old female mice and three 6-week-old male and three female mice) were weighed individually and the wet weight of the spleen and lung was taken. Two independent experiments (n = 3) were performed with each experiment comprising of 3 mice per group. Data was analyzed using GraphPad prism. Data represents mean ± SD. *p<0.05, **p<0.01 and ****p<0.0001.

γMtb treatment did not affect the viability of adult and neonatal mice lung and spleen cells.

Lung and spleen cells from neonatal and adult mice were isolated as mentioned in the methods section and cultured with or without 10µg/ml *γMtb*. After 72 hours, cell viability was measured using lactate dehydrogenase (LDH) assay as described in the methods section. As shown in Fig. 2, there is no difference in the cell viability across all four groups tested. These results indicated that *γMtb* stimulation did not affect the viability of neonatal and adult lung and spleen cells.

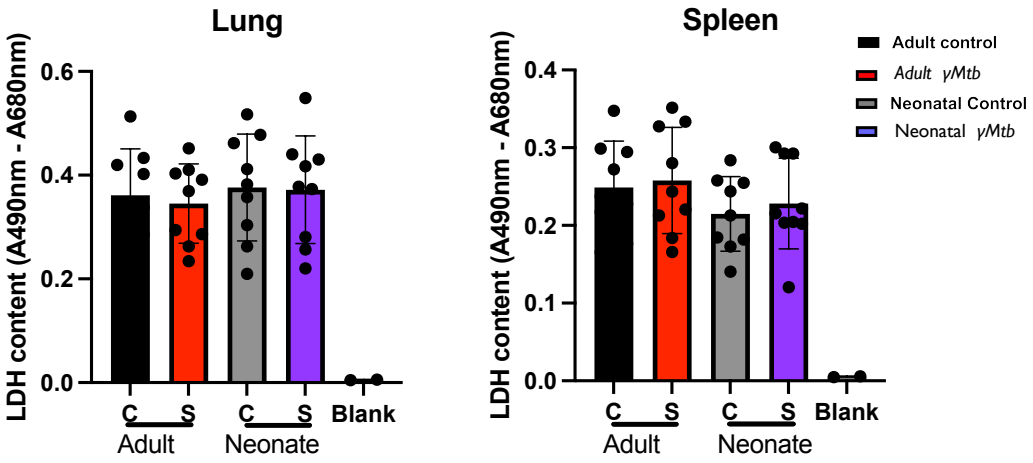

Figure 2: Gamma γ*Mtb* stimulation has no effect on viability of neonatal and adult lung and spleen cells. Lung and spleen cells were isolated from adult and neonatal C57BL/6 mice and cultured in 24 well plate with or without 10 µg/ml γ*Mtb*. After 72 hours cell viability was measured using lactate dehydrogenase assay as mentioned in methods section. Three independent experiments (n = 3) were performed with each experiment comprising of 3 mice per group. Data represents mean ± SD.

Cytokine profile of *γMtb* stimulated neonatal and adult lung cells.

Adult and neonatal mice lung cells were isolated and cultured with or without *γMtb* (10 ng/ml) as described in the methods section. After 72 hours, TNF-*α*, IL-6, IL-10, IL-17A, and IFN-*γ* levels in the culture supernatants were measured by ELISA. As shown in Fig. 3, adult and neonatal lung cells stimulated with *γMtb* produced significantly higher levels of IL-6, TNF-*α*, and IL-10 compared to unstimulated control cells. In addition, we found that neonatal lung cells stimulated with *γMtb* produced significantly higher levels of IL-6, TNF-α, and IL-10 when compared to adult lung cells stimulated with *γMtb* (Fig. 3). IL-17A levels only increased significantly in the stimulated neonatal lung cells when compared to the unstimulated neonatal control.

No difference was found in IFN-*γ* production in neonatal and adult cells with and without *γMtb* stimulation (Fig. 3).

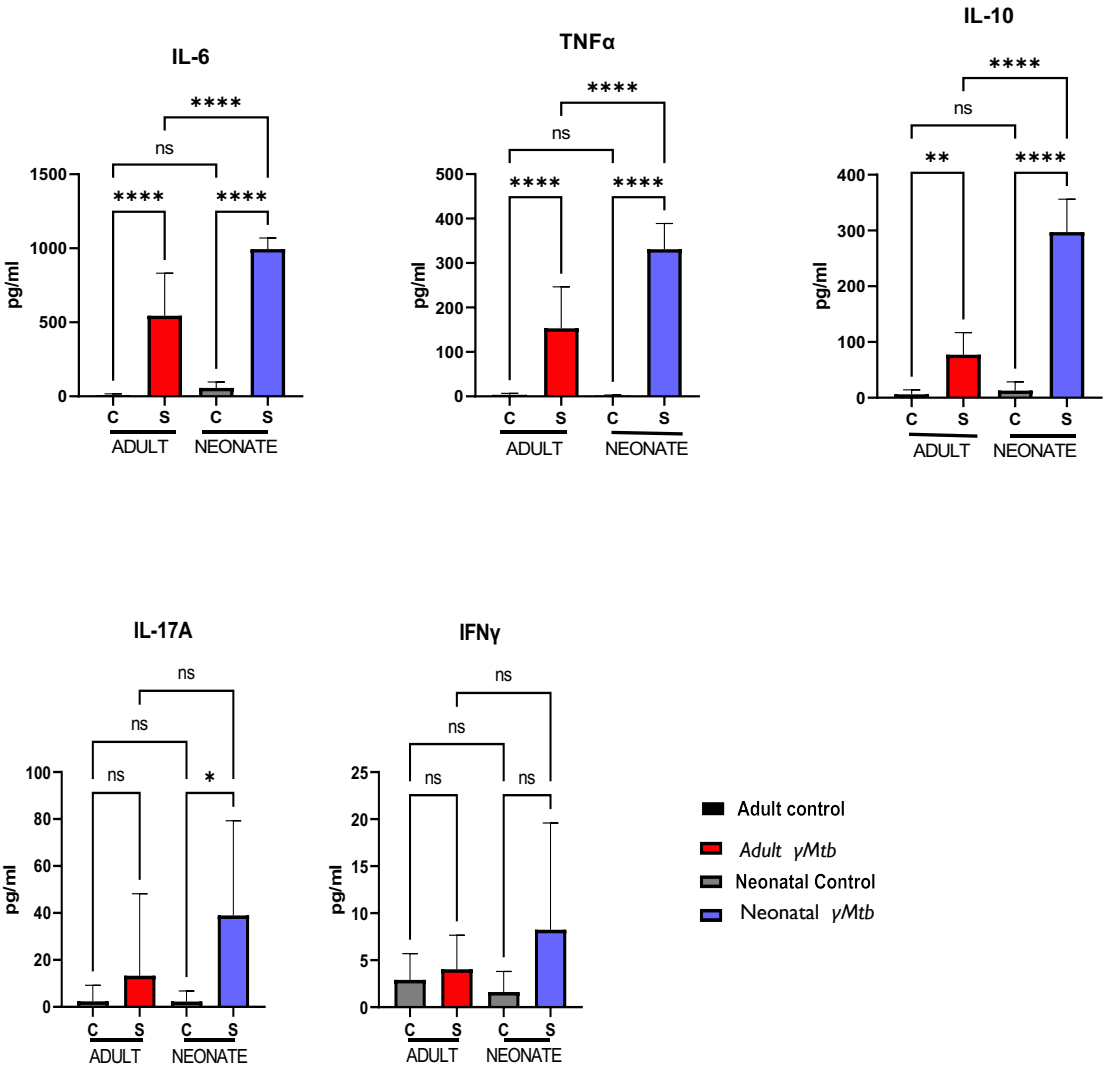

Figure 3: Cytokine profile of γ*Mtb* stimulated adult and neonate lung cells.
Lung cells were isolated from adult and neonatal C57BL/6 mice and cultured in 24 well plate with or without 10 µg/ml *γMtb* for 72 hours. After 72 hours cytokine levels in the supernatant were determined using ELISA. Three independent experiments (n = 3), with each experiment composing of 3 mice per group were performed. Data represents mean ± SD. *P<0.05, **P<0.01 and ****P<0.0001. ns = non-significant.

Cytokine profile of *γMtb* stimulated neonatal and adult spleen cells.

Adult and neonatal mice spleen cells were isolated and stimulated with or without *γMtb* (10 ng/ml) as mentioned in the methods section. After 72 hours, TNF-*α*, IL-6, IL-10, IL-17A, and IFN-*γ* levels in the culture supernatants were measured by ELISA.

As shown in Fig. 4, adult and neonatal spleen cells cultured with *γMtb* produced significantly higher levels of IL-6, TNF-*α,* and IL-10 compared to untreated control cells. However neonatal spleen cells stimulated with *γMtb* produced

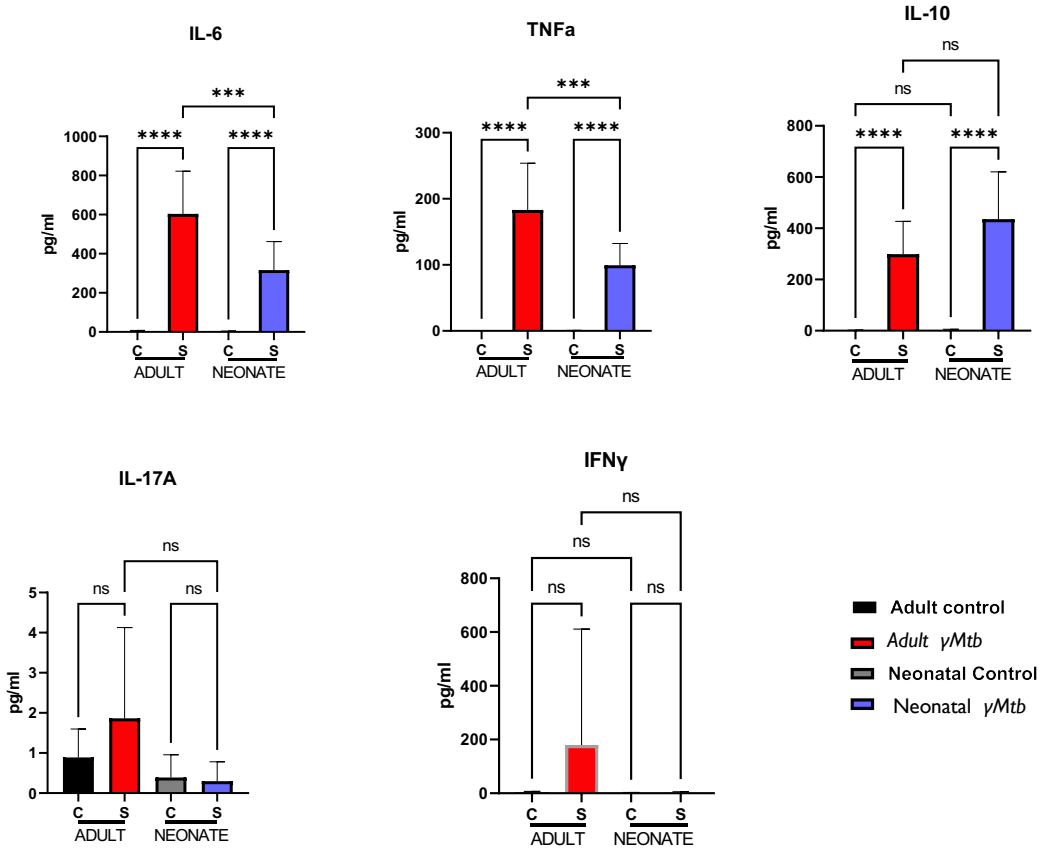

Figure 4: Cytokine profile of γ*Mtb* stimulated adult and neonate spleen cells.
Spleen cells were isolated from adult and neonatal C57BL/6 mice and cultured in 24 well plate with or without 10 µg/ml *γMtb* for 72 hours. After 72 hours cytokine levels in the supernatant were determined using ELISA. Three independent experiments (n = 3), with each experiment composing of 3 mice per group were performed. Data represents mean ± SD. ***P<0.001 and ****P<0.0001. ns = non-significant.

significantly lower levels of IL-6 and TNF-*α* compared to *γMtb*-stimulated adult spleen cells and there is no significant difference in the level of IL-10 between the stimulated groups. *γMtb* stimulation did not affect the IL-17A and INF-*γ* production by adult and neonatal spleen cells compared with untreated control cells (Fig. 4).

Gating Strategy

The flow cytometry gating strategy was designed to accurately identify and quantify distinct immune cell populations in total lung and spleen cells cultured in vitro with medium or *γMtb* for 72 h. The gating strategy was applied to analyze both control and *γMtb* treated samples, for analysis of changes in immune cell populations. Live cells were gated based on forward scatter (FSC) and Aqua Live/Dead stain (VL2-H) to exclude dead cells from the analysis. Then single cells were gated based on forward scatter (FSC-A)/(FSC-H) properties to exclude debris and cells that may have clumped together during the staining process. CD45+ leukocytes were identified as the parent population for subsequent analysis. Specific immune cell subsets were then identified based on their characteristic surface marker expression profiles. These subsets included CD4+ T cells, CD8+ T cells, CD4+CD8+ double-positive cells, NK1.1+ natural killer (NK) cells, MHCII-expressing cells (antigen-presenting cells), B cells, CD11c+ cells, CD11b+ cells.

The percentage and absolute numbers of each immune cell subset were calculated based on the gated populations, providing quantitative data on the composition of immune cell populations in neonatal and adult mice under different experimental conditions.

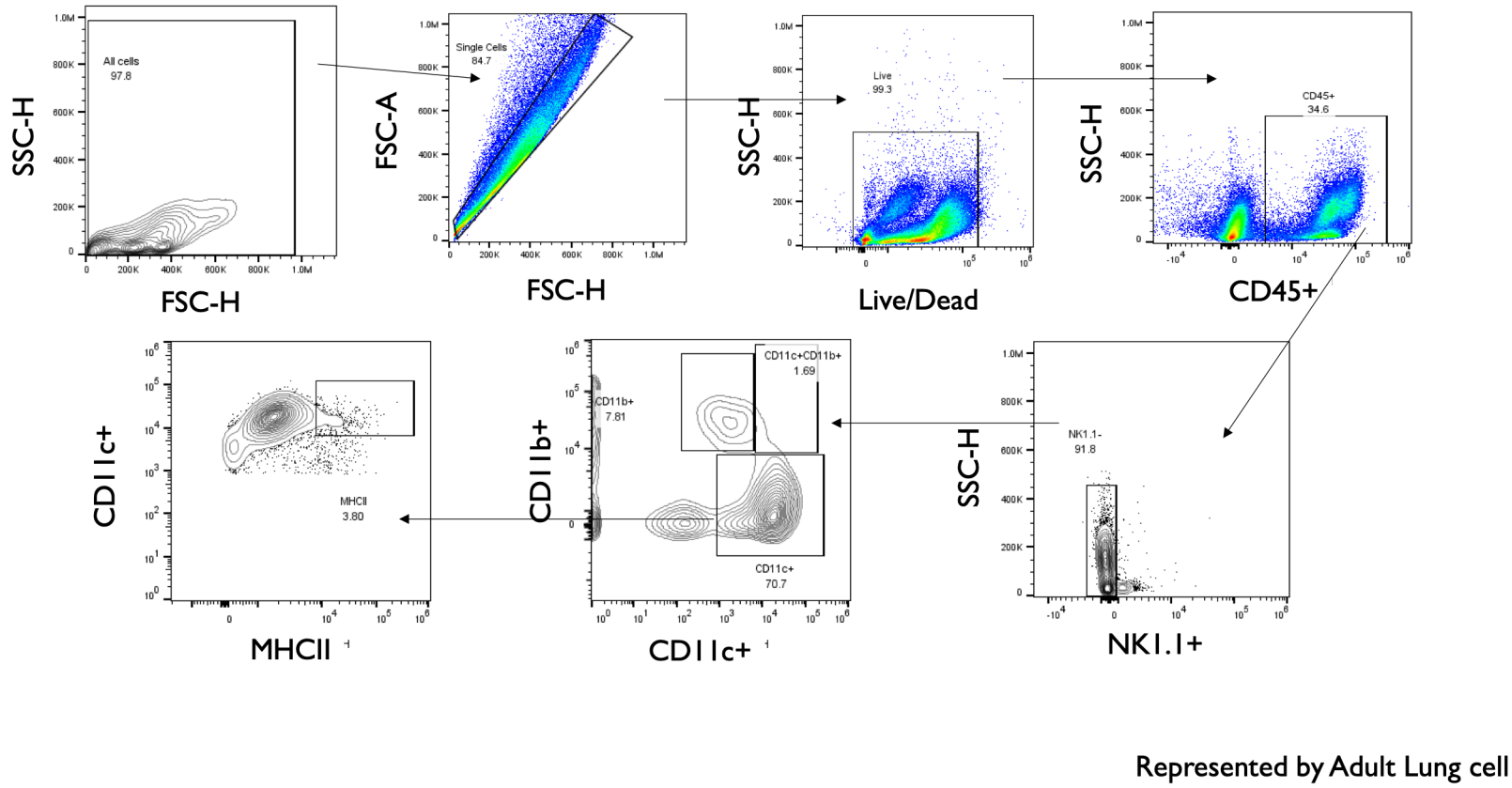

Figure 5: Gating Strategy of Freshly Isolated Myeloid Cell Populations.
Gating strategy for the analysis of myeloid cell populations using Flow Cytometry. Cells were isolated and stained with fluorescent antibodies targeting specific cell surface markers and flow cytometry was performed. Data was analyzed using Flowjo software.

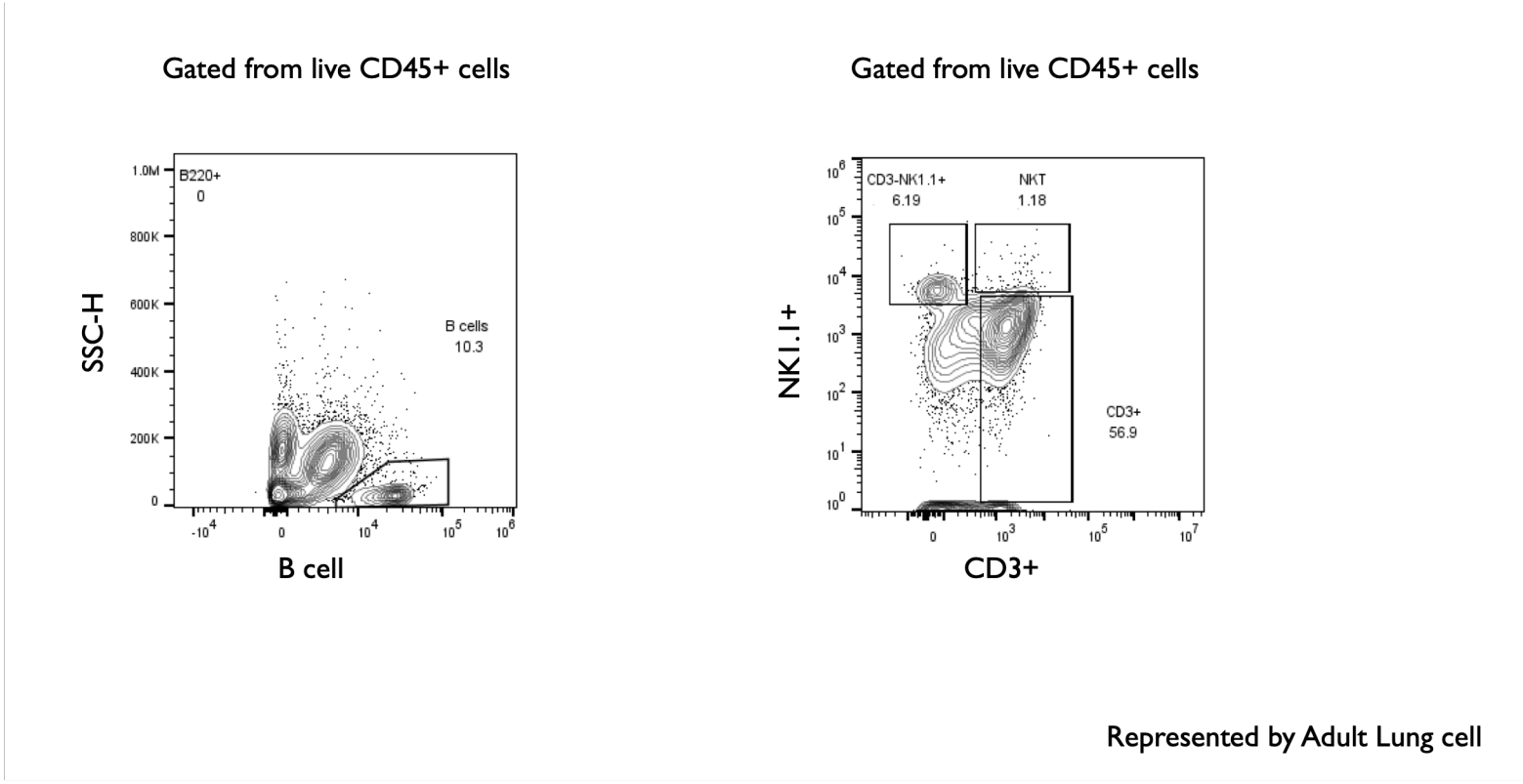

Figure 6: Gating strategy of freshly isolated NK and B cells.
Gating strategy for the analysis of NK and B cell populations using flow cytometry. Cells were isolated and stained with fluorescent antibodies targeting specific cell surface markers and flow cytometry was performed. Data was analyzed using Flowjo software.

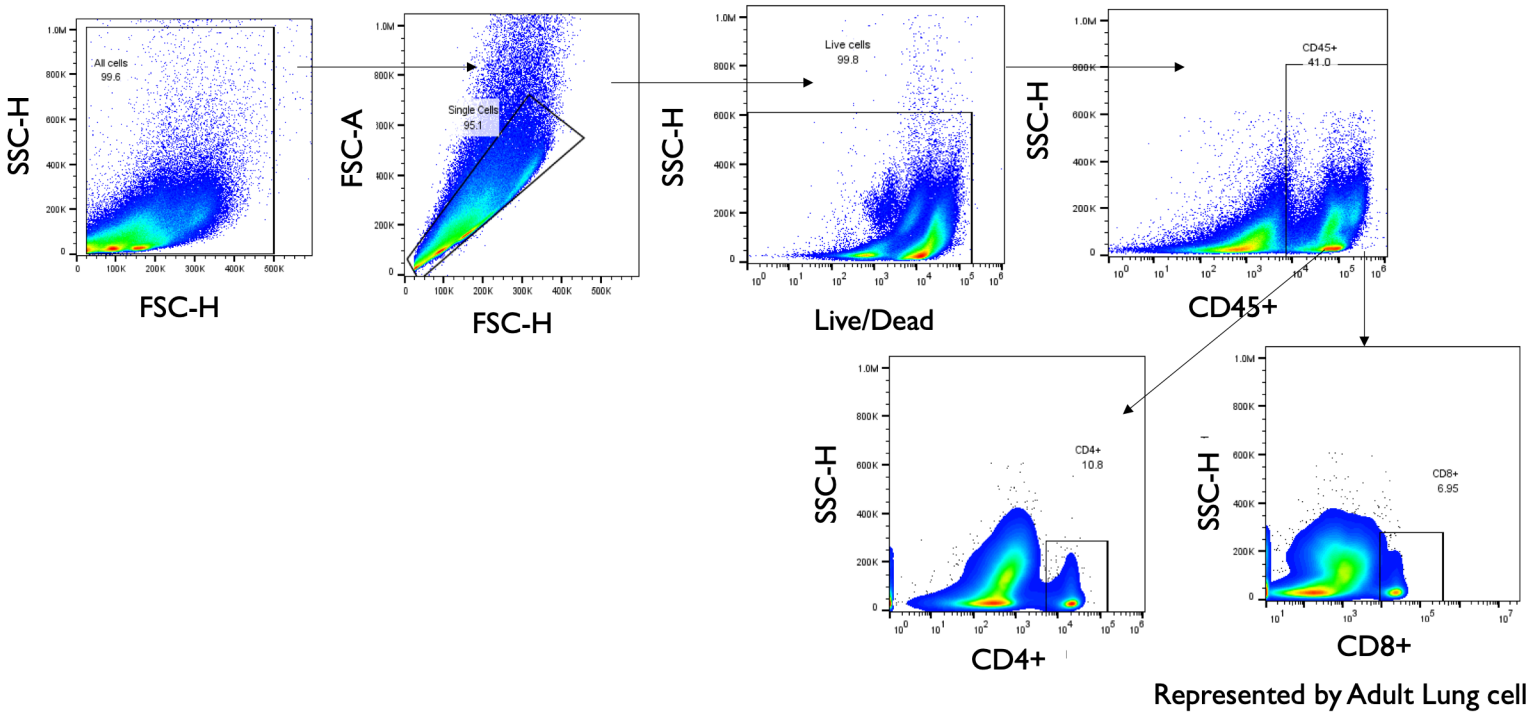

Figure 7: Gating Strategy of freshly isolated T Cells.
Gating strategy for the analysis of T cell populations using flow cytometry. Cells were isolated and stained with fluorescent antibodies targeting specific cell surface markers and flow cytometry was performed. Data was analyzed using Flowjo software.

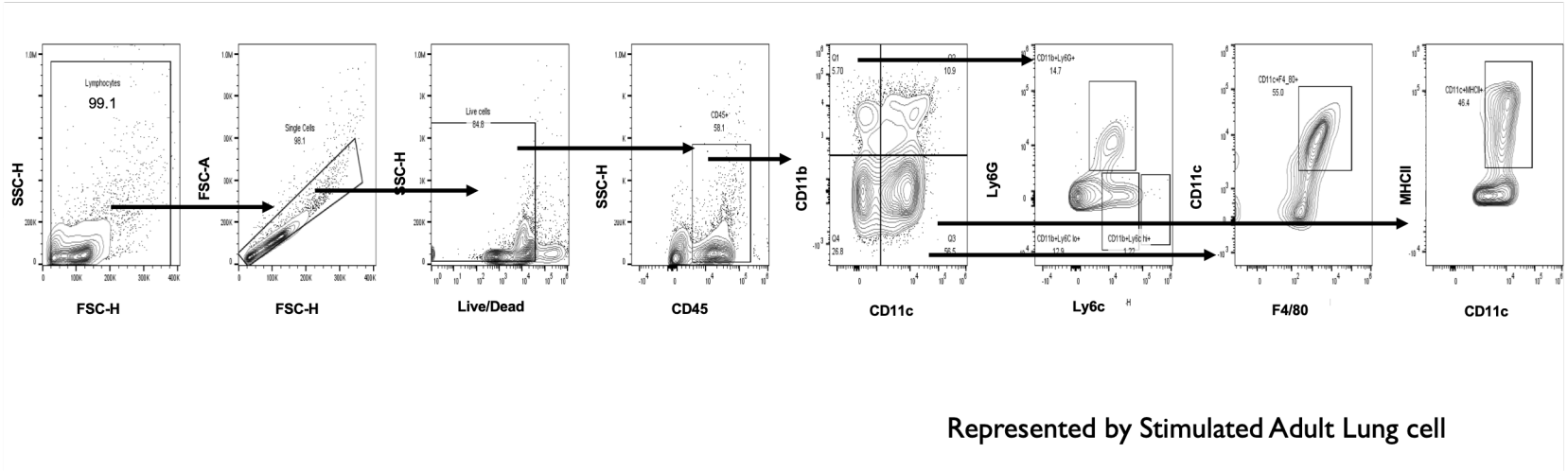

Figure 8: Gating Strategy of *yMtb* stimulated Myeloid Cell Populations.
Gating strategy for the analysis of myeloid cell populations using flow cytometry. Cells were isolated and stained with fluorescent antibodies targeting specific cell surface markers and flow cytometry was performed. Data was analyzed using Flowjo software.

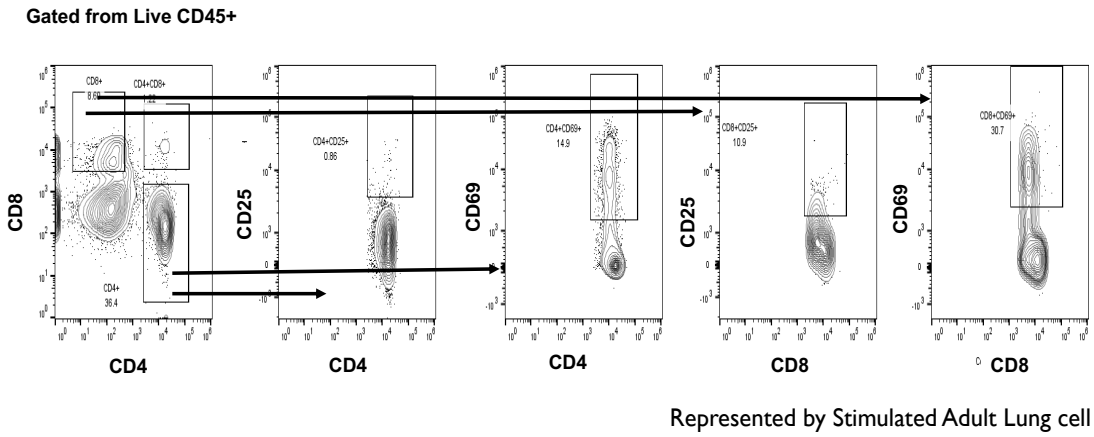

Figure 10: Gating Strategy of *γMtb* stimulated T Cells.
Gating strategy for the analysis of T cell populations using flow cytometry. Cells were isolated and stained with fluorescent antibodies targeting specific cell surface markers and flow cytometry was performed. Data was analyzed using Flowjo software.

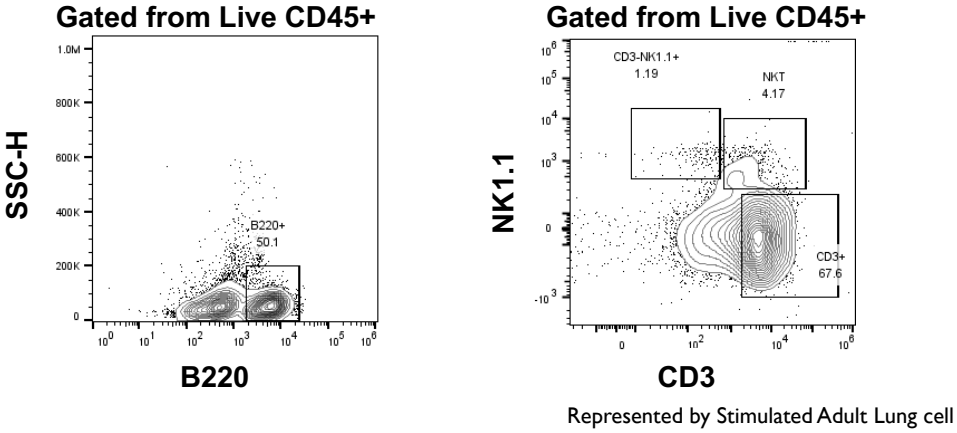

Figure 9: Gating strategy of *γMtb* stimulated NK and B cells.
Gating strategy for the analysis of NK and B cell populations using flow cytometry. Cells were isolated and stained with fluorescent antibodies targeting specific cell surface markers and flow cytometry was performed. Data was analyzed using Flowjo software.

Immune cell profile of freshly isolated adult and neonatal mice lung cells.

Neonatal and adult mice lung cells were isolated as mentioned in the methods section and stained with various surface staining antibodies (Tables. 1-3) to determine the percentages of various immune cell populations. As shown in Fig. 11, the percentage of lung CD45+CD4+CD8+ cells was significantly higher in the neonates when compared with the adults. In contrast, the percentage of CD11c+MHCII+ and NK1.1+ cells were significantly lower in the neonates when compared with the adults, The determined other immune cell populations between both groups were not statistically significant (Fig. 11).

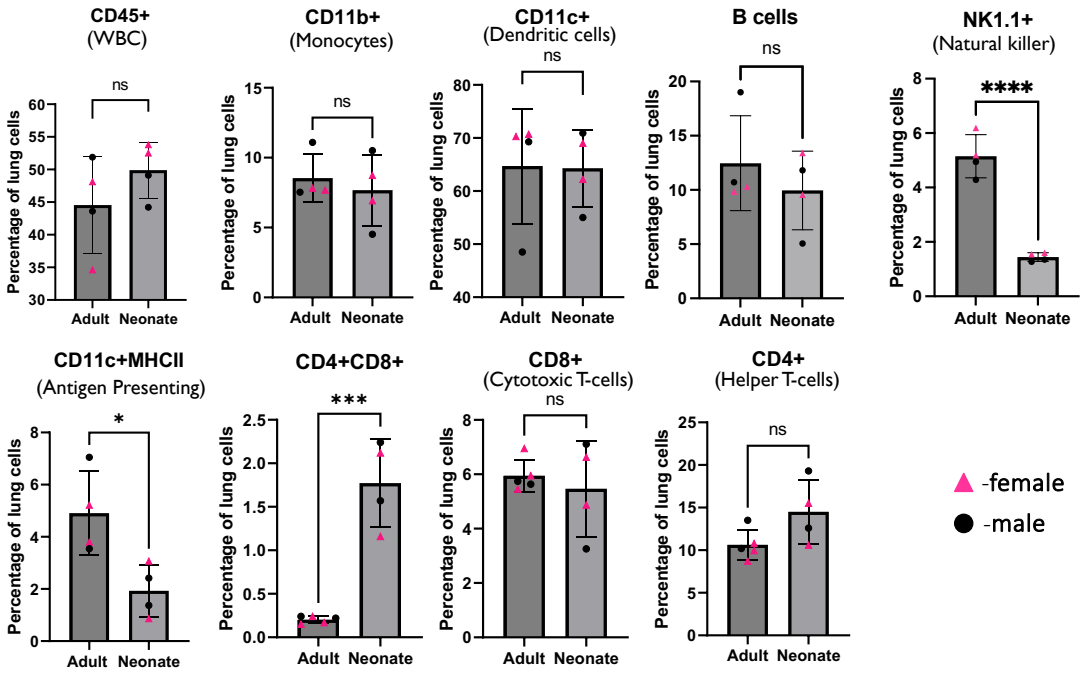

Figure 11: Immune cell profile of freshly isolated adult and neonate lung cells.
Lung cells were isolated from adult and neonatal C57BL/6 mice and were stained with fluorescent antibodies targeting cell type specific surface markers. Cell populations were determined by flow cytometry and data was analyzed using GraphPad Prism. Data represent mean ± SD. *P<0.05, ***P<0.001 and ****P<0.0001. ns = non-significant. (n=4 mice/group)

Immune cell profile of freshly isolated adult and neonatal mice spleen cells.

Neonatal and adult mice spleen cells were isolated and stained with various cell surface staining antibodies (Tables. 1-3) to determine the percentages of various immune cell populations.

As shown in Fig. 12, the percentage of B cells (B220+) and CD11b+ cells were significantly higher in the neonates when compared with the adult cells. The percentage of CD45+, CD8+, CD4+, CD4+CD8+, CD11c+MHCII+, CD11c+CD11b+, and NK1.1+ cells were significantly lower in the neonates when compared with the adult cells and there was no difference in the percentage of CD11c+ between the groups.

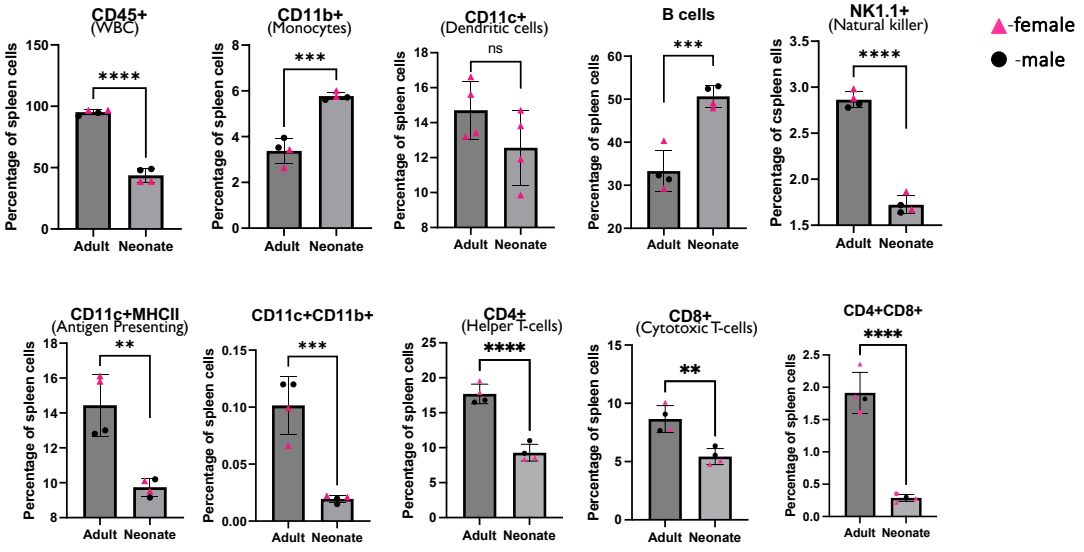

Figure 12: Immune cell profile of freshly isolated adult and neonate spleen cells.
Spleen cells were isolated from adult and neonatal C57BL/6 mice and were stained with fluorescent antibodies targeting cell type specific surface markers. Cell populations were determined by flow cytometry and data was analyzed using GraphPad Prism. Data represent mean ± SD. **P<0.01, ***P<0.001 and ****P<0.0001. ns = non-significant. (n=4 mice/group).

Immune cell profile of *γMtb* stimulated adult and neonatal lung cells.

Neonatal and adult mice lung cells were isolated and cultured, with or without *γMtb* (10μg/ml). After 72 hours, cells were stained with various surface staining antibodies (Tables. 1- 3). In *γMtb* cultured lung cells, the number of CD11b+ cells and NK1.1+ cells were significantly lower and, the number of CD4+, CD4+CD69+, and CD11b+Ly6G+ cells were significantly higher in the neonates when compared with the adults. There is no statistical significance of other cell populations between all the groups tested (Fig. 13).

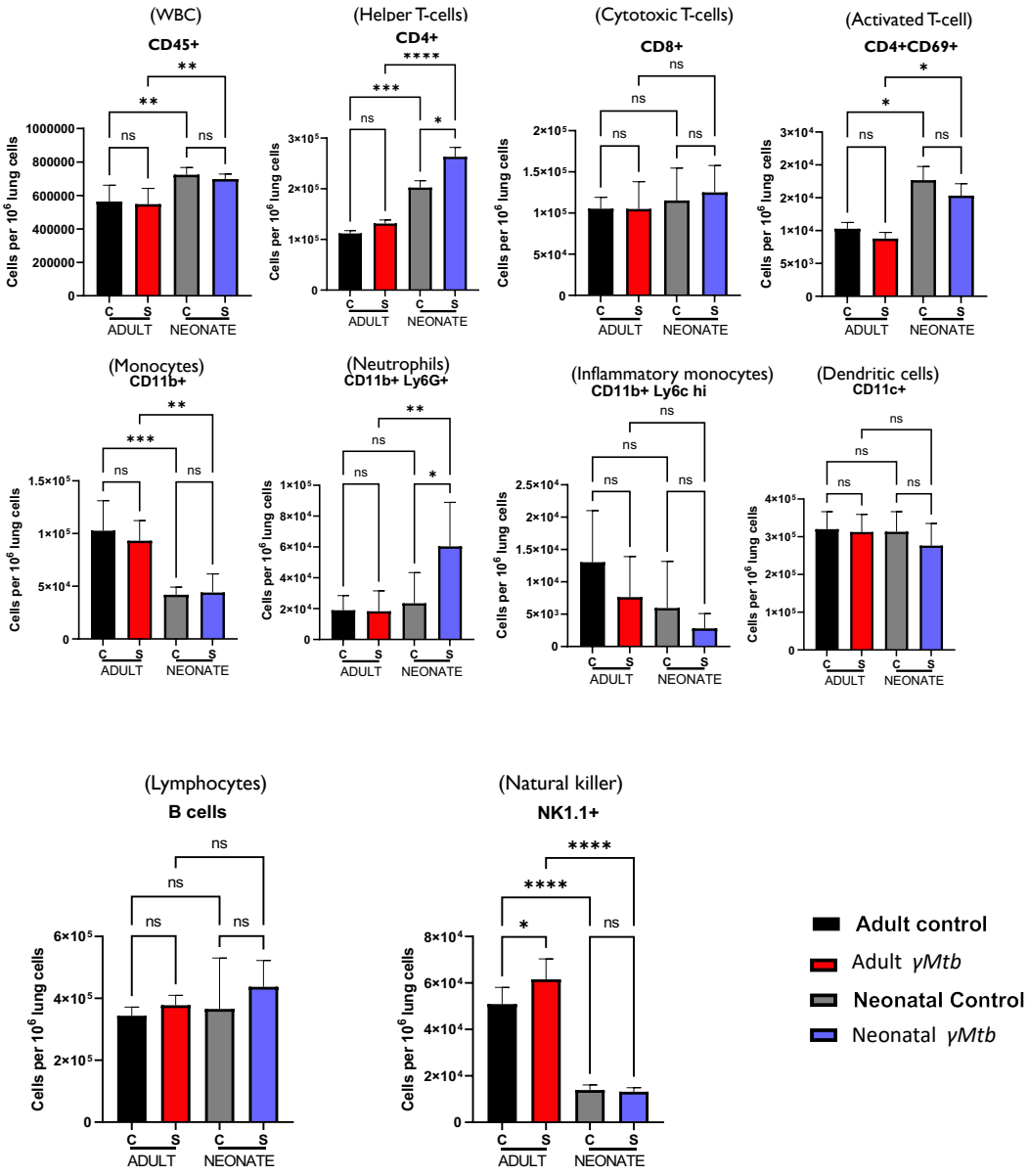

Figure 13: Effect of γ*Mtb* stimulation on lung cells.
Lung cells were isolated from adult and neonatal C57BL/6 mice and cultured in 24 well plate with or without 10 µg/ml *γMtb.* After 72 hours, the cells were stained with respective fluorescent antibodies as mentioned in the methods section. Cell populations was determined by flow cytometry and data was analyzed using GraphPad Prism. Data shown from two independent experiments with each experiment having 3 mice per group. Data shown are mean ± SD. *P<0.05, **P<0.01, ***P<0.001 and ****P<0.0001. ns = non-significant.

Immune cell profile of *γMtb* stimulated adult and neonatal spleen cells

Neonatal and adult mice spleen cells were isolated and cultured, with or without *γMtb* (10μg/ml). After 72 hours, cells were stained with various surface staining antibodies (Tables. 1 - 3). In *γMtb* cultured spleen cells, the number of CD11b+, CD11b+Ly6c hi, and CD11b+CD11c+ cells were significantly higher in the neonates when compared with the adult cells (Fig. 14). The number of CD4+ and NK1.1+ cells was significantly higher in the stimulated neonatal spleen cells when compared with the neonatal unstimulated control cells. B220+ (B cells) cells were significantly lower in the neonates when compared with the adults. Meanwhile, the comparisons between both groups in the other cell populations were not statistically significant (Fig. 14).

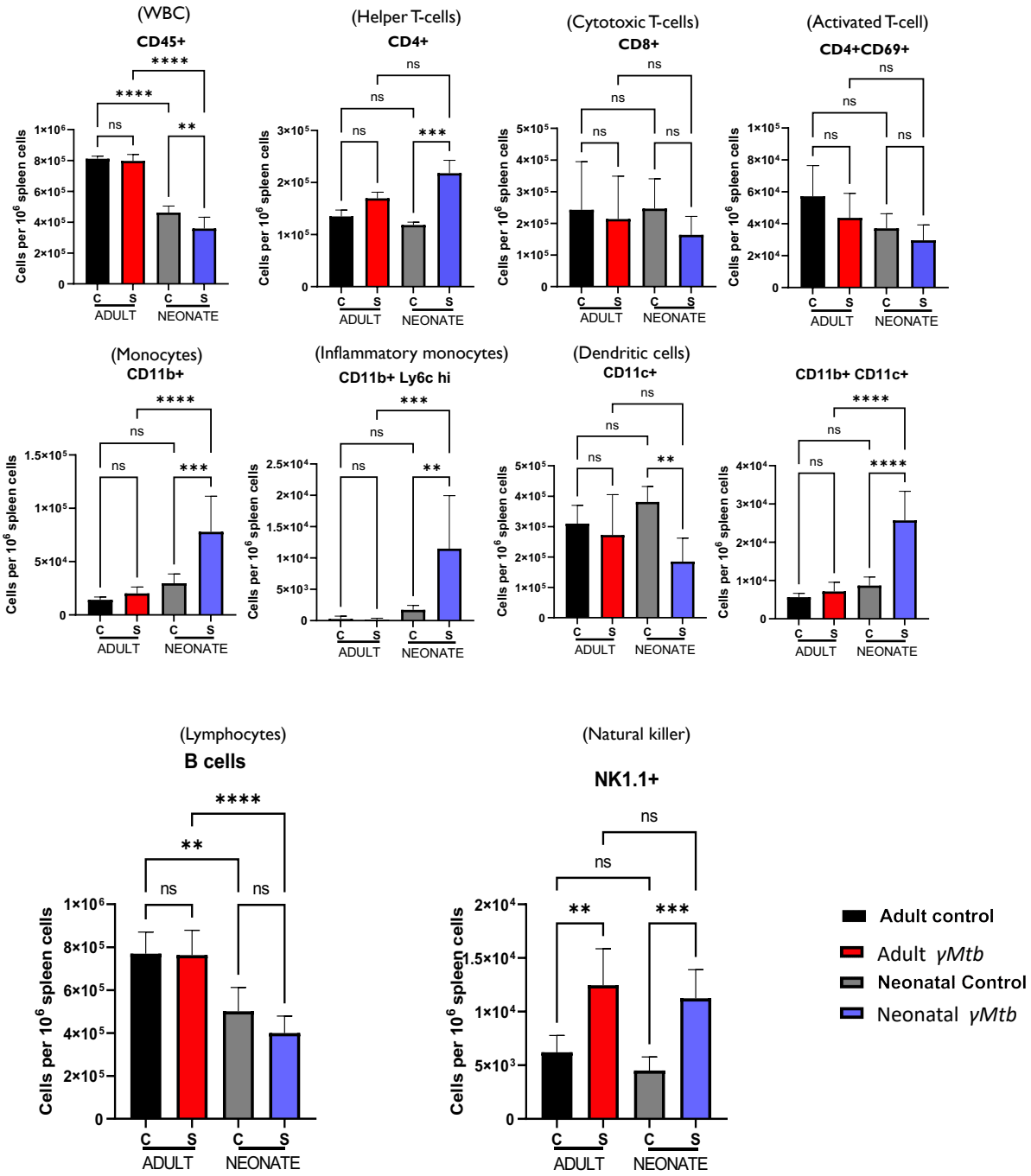

Figure 14: Effect of γ*Mtb* stimulation on spleen cells.
Spleen cells were isolated from adult and neonatal C57BL/6 mice and cultured in 24 well plate with or without 10 µg/ml *γMtb.* After 72 hours, the cells were stained with respective fluorescent antibodies as mentioned in the methods section. Cell populations was determined by flow cytometry and data was analyzed using GraphPad Prism. Data shown from two independent experiments with each experiment having 3 mice per group. Data shown are mean ± SD. **P<0.01, ***P<0.001 and ****P<0.0001. ns = non-significant.

DISCUSSION

Tuberculosis (TB) presents a significant global health challenge, particularly impacting vulnerable populations like neonates with their underdeveloped immune systems. Understanding differences in immune responses to TB infection between neonates and adults is crucial for advancing vaccine development and treatment strategies.

In the current study, we compared the immune responses of neonatal (14-days-old) and adult mice (6-weeks-old) lung and spleen cells in response to *γMtb*. We found significantly higher levels of IL-6, IL-10, and TNF-α in *γMtb* stimulated neonatal lung cell culture supernatants compared to unstimulated controls and adult mice lung cells stimulated with *γMtb*. IL-6 and TNF-α are well-established pro-inflammatory cytokines associated with the host response to tuberculosis infection, playing critical roles in immune defense against mycobacterial pathogens [17]. Conversely, IL-10 is recognized for its anti-inflammatory properties [18] and is often implicated in regulating excessive inflammation and tissue damage during infection [19]. In our study, we found higher levels of IL-10 (Fig. 3) in neonatal lung cells which suggests a potential compensatory mechanism to mitigate the excess inflammatory response triggered by *γMtb* stimulation [20].

Furthermore, our analysis revealed no significant changes in the levels of IFN- γ and IL-17A following *γMtb* stimulation in both neonatal and adult lung cells (Fig. 3). IFN-γ and IL-17A are typically associated with adaptive immune responses and are predominantly produced by memory T cells [21]. The lack of increase in IFN-

γ and IL-17A levels could be because the immune cells utilized in our study consist of naive cells that have not encountered tuberculosis infection previously.

The flow cytometry analysis of freshly isolated lung and spleen cells aimed to characterize the baseline immune cell populations present in neonatal and adult mice before any exposure to tuberculosis (TB) infection or stimulation.

In the lung, our analysis revealed notable differences in the distribution of immune cell populations between neonatal and adult mice. Specifically, neonatal lung cells exhibited a higher percentage of CD4+CD8+ double-positive cells compared to adult lung cells (Fig. 11). CD4+CD8+ double-positive cells represent a subset of T cells that express both CD4+ and CD8+ co-receptors and engage in regulating immune responses [22]. The elevated proportion of CD4+CD8+ double-positive cells in neonatal lungs suggests an altered T cell phenotype characteristic of early life stages, which may impact the immune responses to TB infection [23].

Contrary to T cells, the percentage of MHCII-expressing cells (antigen-presenting cells) and NK1.1+ cells (natural killer cells) were significantly lower in freshly isolated neonatal lung cells compared to adult lung cells (Fig. 11). MHCII-expressing cells, including dendritic cells, macrophages, and B cells [24] play crucial roles in antigen presentation and activation of adaptive immune responses [25]. The reduced proportion of MHCII-expressing cells in neonatal lungs may reflect immaturity in antigen presentation and adaptive immune activation [4] during early life stages, potentially influencing the host defense against TB infection.

In contrast, the flow cytometry analysis of freshly isolated spleen cells revealed different alterations in immune cell populations between neonatal and adult

mice. Neonatal spleen cells exhibited a higher percentage of B cells compared to adult spleen cells (Fig. 12). B cells are integral components of the adaptive immune system, contributing to antibody production and antigen presentation [26]. The increased proportion of B cells in neonatal spleens may indicate a heightened readiness for antibody-mediated immune responses in early life stages, potentially influencing the susceptibility to and control of TB infection [27].

Additionally, freshly isolated neonatal spleen cells showed a higher percentage of CD11b+ cells compared to adult spleen cells (Fig. 12). CD11b+ cells, including macrophages, dendritic cells, and granulocytes [28], are important mediators of innate immune responses and play diverse roles in host defense against pathogens [29]. The elevated proportion of CD11b+ cells in neonatal spleens suggests an enhanced innate immune surveillance capacity [30], which may contribute to the early detection and containment of TB infection in neonates.

Furthermore, the percentage of several immune cell populations, including CD45+ cells (pan-leukocytes), CD8+ T cells, CD4+ T cells, CD4+CD8+ double-positive cells, CD11c+CD11b+ cells, NK1.1+ cells, and CD11c+MHCII+ cells were significantly lower in freshly isolated neonatal spleens compared to adult spleen (Fig. 12). These findings may indicate immaturity in the spleen immune cell composition during early life stages, which could influence the overall immune responses to TB infection in neonates.

The flow cytometry analysis of the cell populations after stimulation with *γMtb* showed differences between neonatal and adult mice. Neonatal lung cells stimulated with *γMtb* exhibited a significantly higher number of CD4+ T cells compared to

stimulated adult mice (Fig. 13). Additionally, the percentage of CD4CD69+ cells, indicative of activated CD4+ T cells [31], was also elevated in stimulated neonates compared to stimulated adults. These findings suggest a robust T cell response in neonates upon exposure to TB antigens, characterized by the activation and expansion of CD4+ T cells in the lung microenvironment. The increased presence of activated CD4+ T cells in neonatal lungs may reflect a heightened immune reactivity to TB infection [32], potentially contributing to enhanced host defense mechanisms against the pathogen.

The absence of a significant increase in CD4+ T cells in the spleens of stimulated neonatal mice compared to stimulated adults may indicate differential immune responses in systemic versus local tissue compartments (Fig. 14). In the lungs, stimulated neonatal mice also exhibited a significantly lower number of NK1.1+ cells compared to stimulated adult mice (Fig. 13). This reduction in NK1.1+ cells suggest a dampened NK cell response upon exposure to TB antigens, potentially reflecting an impaired innate immune surveillance capacity in the lung microenvironment of neonates. Conversely, in the spleens of stimulated neonatal mice, the number of NK1.1+ cells was higher compared to unstimulated neonates. However, this increase was not observed when comparing stimulated neonates to stimulated adults (Fig. 14). The elevated presence of NK1.1+ cells in the spleens of stimulated neonatal mice suggests a potential compensatory response to TB antigens, aimed at strengthening innate immune defenses [33].

Furthermore, the flow cytometry analysis revealed a lower number of B cells in the spleens of unstimulated and stimulated neonatal mice compared to adult mice

spleen cell counterparts (Fig. 14). B cells play critical roles in adaptive immune responses, including antibody production and antigen presentation [26], and their decreased abundance in neonatal spleens following stimulation may reflect altered immune regulatory mechanisms in early life stages [34]. Both unstimulated and stimulated neonatal mice lung cells exhibited a significantly lower number of CD11b+ cells compared to adult mice lung cells, indicating a reduced presence of myeloid cells in the lung microenvironment of neonates (Fig. 13). However, the proportion of lung CD11b+Ly6G+ cells, which typically represent granulocytic myeloid cells such as neutrophils, was higher in neonatal stimulated cells compared to adult stimulated cells (Fig. 13), which is unexpected given that neutrophils, typically do not increase in number due to their short lifespan [35]. This suggests a potential phenomenon of phenotypic plasticity [36], wherein neutrophils acquire the phenotype of other cell types or populations under specific conditions [37], such as exposure to *γMtb*. Notably, confirming the precise phenotype of CD11b+ cells observed in this study is a limitation. Further investigation on isolating the CD11b+ cell population after *γMtb* stimulation and subsequent morphological and functional studies would ascertain the specific mechanisms in response to neonatal TB infection.

The observed increase in lung CD11b+Ly6G+ cells in neonatal stimulated cells compared to adult stimulated cells (Fig. 13), is given to its important potential implications for the host response to TB infection. Neutrophils are pivotal effectors of the innate immune response, tasked with combating microbial threats through phagocytosis and the release of antimicrobial molecules [38] [39]. Depletion of CD11b+Ly6G+ cells has been reported to result in a dramatic increase in tissue

damage at the site of infection [40]. Therefore, the observed higher abundance of CD11b+Ly6G+ cells in neonatal stimulated cells could suggest a more robust neutrophil-mediated host defense mechanism in neonates compared to adults, potentially contributing to the containment of TB infection, and limiting tissue damage. In the spleen, stimulated neonatal mice exhibited a higher number of CD11b+ cells compared to stimulated adult mice (Fig. 14), suggesting an enhanced presence of myeloid cells in the spleen microenvironment of neonates in response to TB antigens. Additionally, the proportions of CD11b+Ly6c hi and CD11b+CD11c+ cells were higher in neonatal stimulated spleen cells compared to adult stimulated spleen cells (Fig. 14), indicative of an altered composition of myeloid cell subsets in neonates following TB antigen exposure. Conversely, the number of CD11c+ cells was lower in neonatal stimulated spleen cells compared to neonatal unstimulated spleen cells, suggesting a potential suppression of dendritic cell populations in neonatal spleen following TB antigen stimulation (Fig. 14).

In summary, this study provides valuable insights into the complex dynamics of immune responses to tuberculosis (TB) infection in neonatal and adult mice. By comparing the immune profiles of lung and spleen cells between neonates and adults following *γMtb* stimulation, we identified differences in cytokine secretion and immune cell composition. Neonates exhibited distinct patterns of immune cell distribution and cytokine responses, indicating age-related variations in host immune profiles. Despite the challenges posed by neonatal immaturity, such as reduced antigen presentation and diminished innate immune surveillance, our data suggest potential compensatory mechanisms and heightened immune reactivity in neonates

upon TB antigen exposure. Moreover, the observed phenotypic plasticity in myeloid cell populations highlights the intricate nature of host immune responses to TB infection. Overall, our study contributes to a deeper understanding of neonatal immune responses to TB, offering insights that may inform the development of targeted interventions to combat TB in vulnerable populations.

REFERENCES

, [1] M. Schito *et al.*, "Perspectives on Advances in Tuberculosis Diagnostics, Drugs, and Vaccines," *Clin Infect Dis,* vol. 61Suppl 3, no. Suppl 3, pp. S102-18, Oct 15 2015, doi: 10.1093/cid/civ609.

[2] A. M. Cooper, "Cell-mediated immune responses in tuberculosis," *Annu Rev Immunol,* vol. 27, pp. 393-422, 2009, doi: 10.1146/annurev.immunol.021908.132703.

[3] P. J. Busse and S. K. Mathur, "Age-related changes in immune function: effect on airway inflammation," *J Allergy Clin Immunol,* vol. 126, no. 4, pp. 690-9; quiz 700-1, Oct 2010, doi: 10.1016/j.jaci.2010.08.011.

[4] S. M. Newton, A. J. Brent, S. Anderson, E. Whittaker, and B. Kampmann, "Paediatric tuberculosis," *Lancet Infect Dis,* vol. 8, no. 8, pp. 498-510, Aug 2008, doi: 10.1016/S1473-3099(08)70182-8.

[5] G. S. Lamb and J. R. Starke, "Tuberculosis in Infants and Children," *Microbiol Spectr,* vol. 5, no. 2, Apr 2017, doi: 10.1128/microbiolspec.TNMI7-0037-2016.

[6] T. O. Togun, E. MacLean, B. Kampmann, and M. Pai, "Biomarkers for diagnosis of childhood tuberculosis: A systematic review," *PLoS One,* vol. 13, no. 9, p. e0204029, 2018, doi: 10.1371/journal.pone.0204029.

[7] F. W. Basile, P. Nabeta, M. Ruhwald, and R. Song, "Pediatric Tuberculosis Diagnostics: Present and Future," *J Pediatric Infect Dis Soc,* vol. 11, no. Supplement_3, pp. S85-S93, Oct 31 2022, doi: 10.1093/jpids/piac082.

[8] L. Ramos, J. K. Lunney, and M. Gonzalez-Juarrero, "Neonatal and infant immunity for tuberculosis vaccine development: importance of age-matched animal models," *Dis Model Mech,* vol. 13, no. 9, Sep 15 2020, doi: 10.1242/dmm.045740.

[9] A. M. Garcia, S. A. Fadel, S. Cao, and M. Sarzotti, "T cell immunity in neonates," *Immunol Res,* vol. 22, no. 2-3, pp. 177-90, 2000, doi: 10.1385/IR:22:2-3:177.

[10] S. Basha, N. Surendran, and M. Pichichero, "Immune responses in neonates," *Expert Rev Clin Immunol,* vol. 10, no. 9, pp. 1171-84, Sep 2014, doi: 10.1586/1744666X.2014.942288.

[11] J. A. Seddon, S. S. Chiang, H. Esmail, and A. K. Coussens, "The Wonder Years: What Can Primary School Children Teach Us About Immunity to

Mycobacterium tuberculosis?," *Front Immunol,* vol. 9, p. 2946, 2018, doi: 10.3389/fimmu.2018.02946.

[12] G. Arango Duque and A. Descoteaux, "Macrophage cytokines: involvement in immunity and infectious diseases," *Front Immunol,* vol. 5, p. 491, 2014, doi: 10.3389/fimmu.2014.00491.

[13] J. R. Foster, "The functions of cytokines and their uses in toxicology," *Int J Exp Pathol,* vol. 82, no. 3, pp. 171-92, Jun 2001, doi: 10.1046/j.1365-2613.2001.iep0082-0171-x.

[14] Y. V. Cavalcanti, M. C. Brelaz, J. K. Neves, J. C. Ferraz, and V. R. Pereira, "Role of TNF-Alpha, IFN-Gamma, and IL-10 in the Development of Pulmonary Tuberculosis," *Pulm Med,* vol. 2012, p. 745483, 2012, doi: 10.1155/2012/745483.

[15] A. M. Cooper and S. A. Khader, "The role of cytokines in the initiation, expansion, and control of cellular immunity to tuberculosis," *Immunol Rev,* vol. 226, pp. 191-204, Dec 2008, doi: 10.1111/j.1600-065X.2008.00702.x.

[16] A. Goenka *et al.*, "Infant Alveolar Macrophages Are Unable to Effectively Contain Mycobacterium tuberculosis," *Front Immunol,* vol. 11, p. 486, 2020, doi: 10.3389/fimmu.2020.00486.

[17] F. G. Boni, I. Hamdi, L. M. Koundi, K. Shrestha, and J. Xie, "Cytokine storm in tuberculosis and IL-6 involvement," *Infect Genet Evol,* vol. 97, p. 105166, Jan 2022, doi: 10.1016/j.meegid.2021.105166.

[18] K. N. Couper, D. G. Blount, and E. M. Riley, "IL-10: the master regulator of immunity to infection," *J Immunol,* vol. 180, no. 9, pp. 5771-7, May 1 2008, doi: 10.4049/jimmunol.180.9.5771.

[19] J. M. Rojas, M. Avia, V. Martin, and N. Sevilla, "IL-10: A Multifunctional Cytokine in Viral Infections," *J Immunol Res,* vol. 2017, p. 6104054, 2017, doi: 10.1155/2017/6104054.

[20] S. S. Iyer and G. Cheng, "Role of interleukin 10 transcriptional regulation in inflammation and autoimmune disease," *Crit Rev Immunol,* vol. 32, no. 1, pp. 23-63, 2012, doi: 10.1615/critrevimmunol.v32.i1.30.

[21] K. N. McCarthy, S. Hone, R. M. McLoughlin, and K. H. G. Mills, "IL-17 and IFN-gamma-producing respiratory tissue resident memory CD4 T cells persist for decades in adults immunized as children with whole cell pertussis vaccines," *J Infect Dis,* Jan 30 2024, doi: 10.1093/infdis/jiae034.

[22] A. Waschbisch *et al.*, "Analysis of CD4+ CD8+ double-positive T cells in blood, cerebrospinal fluid and multiple sclerosis lesions," *Clin Exp Immunol,* vol. 177, no. 2, pp. 404-11, Aug 2014, doi: 10.1111/cei.12345.

[23] Y. Parel and C. Chizzolini, "CD4+ CD8+ double positive (DP) T cells in health and disease," *Autoimmun Rev,* vol. 3, no. 3, pp. 215-20, Mar 2004, doi: 10.1016/j.autrev.2003.09.001.

[24] K. J. Cho and P. A. Roche, "Regulation of MHC Class II-Peptide Complex Expression by Ubiquitination," *Front Immunol,* vol. 4, p. 369, Nov 13 2013, doi: 10.3389/fimmu.2013.00369.

[25] T. M. Holling, E. Schooten, and P. J. van Den Elsen, "Function and regulation of MHC class II molecules in T-lymphocytes: of mice and men," *Hum Immunol,* vol. 65, no. 4, pp. 282-90, Apr 2004, doi: 10.1016/j.humimm.2004.01.005.

[26] I. Rastogi, D. Jeon, J. E. Moseman, A. Muralidhar, H. K. Potluri, and D. G. McNeel, "Role of B cells as antigen presenting cells," *Front Immunol,* vol. 13, p. 954936, 2022, doi: 10.3389/fimmu.2022.954936.

[27] A. G. Loxton, "Bcells and their regulatory functions during Tuberculosis: Latency and active disease," *Mol Immunol,* vol. 111, pp. 145-151, Jul 2019, doi: 10.1016/j.molimm.2019.04.012.

[28] K. Vermaelen and R. Pauwels, "Accurate and simple discrimination of mouse pulmonary dendritic cell and macrophage populations by flow cytometry: methodology and new insights," *Cytometry A,* vol. 61, no. 2, pp. 170-77, Oct 2004, doi: 10.1002/cyto.a.20064.

[29] G. Lauvau, P. Loke, and T. M. Hohl, "Monocyte-mediated defense against bacteria, fungi, and parasites," *Semin Immunol,* vol. 27, no. 6, pp. 397-409, Dec 2015, doi: 10.1016/j.smim.2016.03.014.

[30] S. Pahari *et al.*, "Reinforcing the Functionality of Mononuclear Phagocyte System to Control Tuberculosis," *Front Immunol,* vol. 9, p. 193, 2018, doi: 10.3389/fimmu.2018.00193.

[31] K. Radulovic, V. Rossini, C. Manta, K. Holzmann, H. A. Kestler, and J. H. Niess, "The early activation marker CD69 regulates the expression of chemokines and CD4 T cell accumulation in intestine," *PLoS One,* vol. 8, no. 6, p. e65413, 2013, doi: 10.1371/journal.pone.0065413.

[32] S. Srivastava and J. D. Ernst, "Cutting edge: Direct recognition of infected cells by CD4 T cells is required for control of intracellular Mycobacterium tuberculosis in vivo," *J Immunol,* vol. 191, no. 3, pp. 1016-20, Aug 1 2013, doi: 10.4049/jimmunol.1301236.

[33] W. M. Yokoyama, "Natural killer cell immune responses," *Immunol Res,* vol. 32, no. 1-3, pp. 317-25, 2005, doi: 10.1385/IR:32:1-3:317.

[34] J. G. Cyster and C. D. C. Allen, "B Cell Responses: Cell Interaction Dynamics and Decisions," *Cell,* vol. 177, no. 3, pp. 524-540, Apr 18 2019, doi: 10.1016/j.cell.2019.03.016.

[35] J. Pillay *et al.*, "In vivo labeling with 2H2O reveals a human neutrophil lifespan of 5.4 days," *Blood,* vol. 116, no. 4, pp. 625-7, Jul 29 2010, doi: 10.1182/blood-2010-01-259028.

[36] J. Y. Sagiv *et al.*, "Phenotypic diversity and plasticity in circulating neutrophil subpopulations in cancer," *Cell Rep,* vol. 10, no. 4, pp. 562-73, Feb 3 2015, doi: 10.1016/j.celrep.2014.12.039.

[37] A. S. McLaren, R. Fetit, C. S. Wood, J. Falconer, and C. W. Steele, "Single cell sequencing of neutrophils demonstrates phenotypic heterogeneity and functional plasticity in health, disease, and cancer," *Chin Clin Oncol,* vol. 12, no. 2, p. 18, Apr 2023, doi: 10.21037/cco-22-121.

[38] C. Rosales, "Neutrophils at the crossroads of innate and adaptive immunity," *J Leukoc Biol,* vol. 108, no. 1, pp. 377-396, Jul 2020, doi: 10.1002/JLB.4MIR0220-574RR.

[39] L. Fingerhut, G. Dolz, and N. de Buhr, "What Is the Evolutionary Fingerprint in Neutrophil Granulocytes?," *Int J Mol Sci,* vol. 21, no. 12, Jun 25 2020, doi: 10.3390/ijms21124523.

[40] M. A. Fischer *et al.*, "CD11b(+), Ly6G(+) cells produce type I interferon and exhibit tissue protective properties following peripheral virus infection," *PLoS Pathog,* vol. 7, no. 11, p. e1002374, Nov 2011, doi: 10.1371/journal.ppat.1002374.

VITA

Oyinkansola Adeyemi entered the University of Lagos, Nigeria as a Bachelors student majoring in Genetics. She graduated with a Bachelor of Science in Cell Biology and Genetics in May 2019. In August of 2022, she entered into the Biotechnology graduate program at the University of Texas Health Science Center at Tyler where she performed her thesis work in the lab of Ramakrishna Vankayalapati, Ph.D.

This thesis was typed by Oyinkansola F. Adeyemi